A R T I C L E

Contribution of the intramolecular hydrogen bond to the shift of the pKa value and the oxidation potential of phenols and phenolate anions†

Daisuke Kanamori, Atsushi Furukawa, Taka-aki Okamura, Hitoshi Yamamoto and Norikazu Ueyama*

Department of Macromolecular Science, Graduate School of Science, Osaka University, Toyonaka, Osaka, 560-0043, Japan. E-mail: ueyama@chem.sci.osaka-u.ac.jp
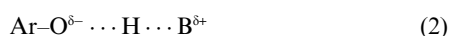
Intramolecularly OH · · · O=C hydrogen bonded phenols, 2-HO–C_6H_2-3,5-(t-Bu)$_2$–CONH–t-Bu (**1–OH**), 2-HO–C_6H_2-5-t-Bu-1,3-(CONH-t-Bu)$_2$ (**2–OH**) and 2-HO–C_6H_2-3,5-(t-Bu)$_2$–NHCO–t-Bu (**4–OH**), were synthesized and their phenolate anions were prepared as tetraethylammonium salts (**1–O⁻ (NEt₄⁺)**, **2–O⁻ (NEt₄⁺)** and **4–O⁻ (NEt₄⁺)**) with intramolecular NH · · · O(oxyanion) hydrogen bonds. 4-HO–C_6H_2-3,5-t-Bu$_2$–CONH–t-Bu (**3–OH**) and its phenolate anion, **3–O⁻ (NEt₄⁺)**, were synthesized as non-hydrogen bonded references. The presence of intramolecular hydrogen bonds was established through the crystallographic analysis and/or ¹H NMR spectroscopic results. Intramolecular NH · · · O(phenol) hydrogen bonds shift the pKa of the phenol to a more acidic value. The results of cyclic voltammetry show that the intramolecular OH · · · O=C hydrogen bond negatively shifts the oxidation potential of the phenol. In contrast, the intramolecular NH · · · O(oxyanion) hydrogen bond positively shifts the oxidation potential of the phenolate anion, preventing oxidation. These contributions of the hydrogen bond to the pKa value and the oxidation potentials probably play an important role in the formation of a tyrosyl radical in photosystem II.

Introduction

The oxidation process of tyrosine is of much interest because of its importance in various enzymes.[1,2] In many of the enzymes containing a tyrosine residue, the formation of a hydrogen bond to the tyrosyl radical has been implied.[3–7] Among these enzymes, much attention has been focused on photosystem II (PSII), in which proton-coupled electron transfer (PCET) occurs (Scheme 1). Studies conducted on model compounds of PSII show that the hydrogen bond promotes the oxidation of phenol and contributes to PCET.[8–11] The model compounds used in these studies realize the OH · · · N hydrogen bond between the tyrosine and histidine residues. The hydrogen bond acceptors in the models are basic substituents such as primary and tertiary amines. Because of the high basicity of the substituents, the model systems are in acid–base equilibrium and probably show an averaged character (2, below). It seems difficult to discuss precisely the contribution of the hydrogen bond under such an equilibrium. In this paper, we present new models that realize two extreme situations (1) and (3), involving phenols with a weakly basic hydrogen bond acceptor and phenolate anions with a weakly acidic hydrogen bond donor. In these models, the contribution of a hydrogen bond to the oxidation of phenols and phenolate anions can be discussed individually. The contribution of the hydrogen bonds to pKa values is also discussed. The acidity of the tyrosine in PSII is one of the most important factors for PCET because it relates to the degree of dissociation of the phenolic proton.

$$\text{Ar–O–H} \cdots \text{B} \qquad (1)$$

$$\text{Ar–O}^{\delta-} \cdots \text{H} \cdots \text{B}^{\delta+} \qquad (2)$$

$$\text{Ar–O}^- \cdots \text{H–B}^+ \qquad (3)$$
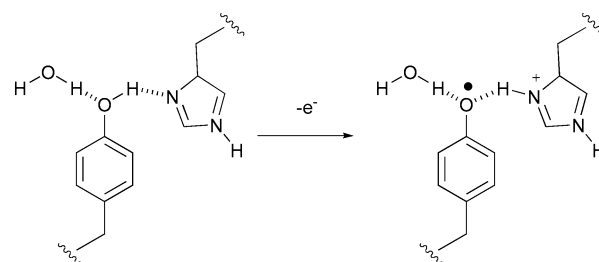
Scheme 1 Proton-coupled electron transfer in photosystem II.

We have recently demonstrated the conformational switching in salicylamide derivatives between the phenol and the phenolate anion (Scheme 2).[12,13] In the phenol, salicylamide derivatives form an intramolecular OH · · · O=C hydrogen bond. In contrast, they form an intramolecular NH · · · O(oxyanion) hydrogen bond in the phenolate anion. We synthesized the phenols shown in Chart 1 as well as their phenolate anions, which are adequate models for systematically discussing the contribution of the hydrogen bond (details of these syntheses are in the supplementary information). *ortho*-Substituted phenols, **1–OH**, **2–OH** and **4–OH**, and their phenolate anions as tetraethylammonium salts, **1–O⁻ (NEt₄⁺)**, **2–O⁻ (NEt₄⁺)** and **4–O⁻ (NEt₄⁺)**, were used as hydrogen-bonding models. In **2–OH** and **2–O⁻ (NEt₄⁺)**, the formation of an additional intramolecular hydrogen bond is expected. Using these models enables us to discuss the contribution of hydrogen bonded water to tyrosine in PSII to the oxidation of the tyrosine. *para*-Substituted isomers, **3–OH** and **3–O⁻ (NEt₄⁺)**, were employed as non-hydrogen bonded references.
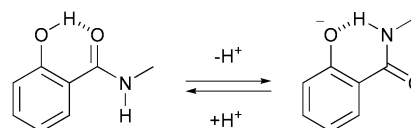
Scheme 2 Conformational switching in salicylamide derivatives in solution.
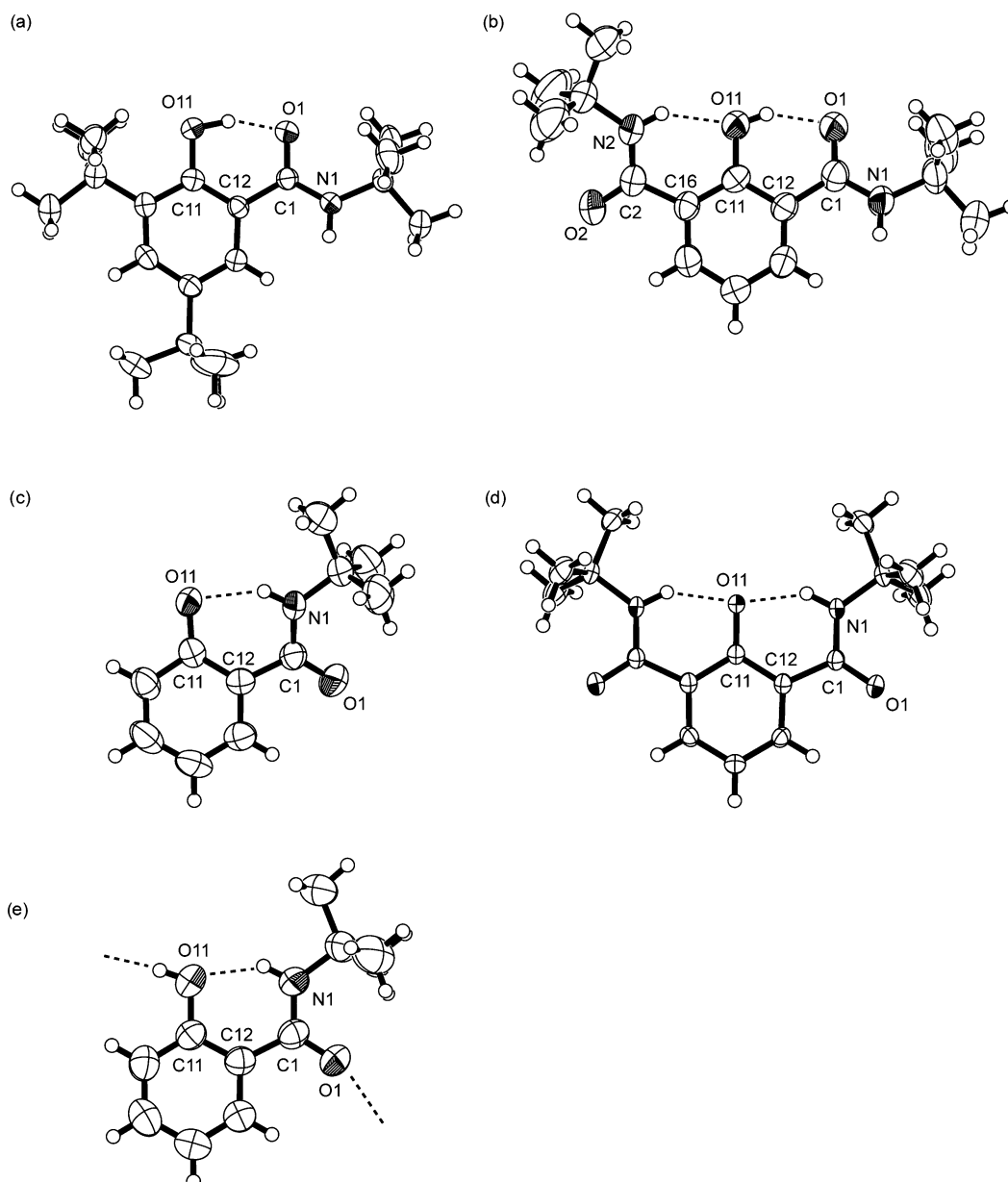
Fig. 1 ORTEP drawings of crystal structures of (a) **1–OH**, (b) **2′–OH**, (c) anion part of **1′–O⁻(NEt₄⁺)·(H₂O)**, (d) anion part of **2′–O⁻(NMe₄⁺)** and (e) **1–OH**.
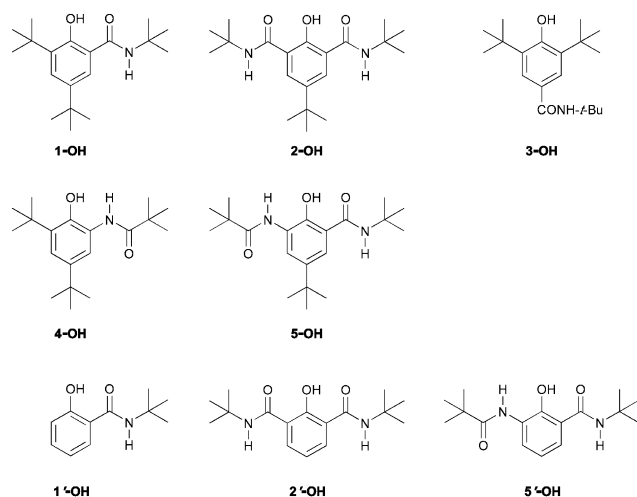
Chart 1

Results and discussion

Crystal structures

The crystal structures of hydrogen bonded phenols and phenolate anions are shown in Fig. 1. The selected short contacts, bond lengths and torsion angles are listed in Table 1. The short distance between phenolic (O11) and carbonyl oxygen (O1) in **1–OH** indicates the presence of an intramolecular OH · · · O=C hydrogen bond. In **2′–OH**, which has two *N-tert*-butylcarbamoyl groups at *ortho*-positions from the phenolic hydroxyl group, one of these groups forms an intramolecular OH · · · O=C hydrogen bond similar to **1–OH**, and the other forms an intramolecular NH · · · O hydrogen bond. In the phenolate anions, short contacts between phenoxy oxygen (O11) and carbamoyl nitrogen (N1) (2.690(4) in **1′–O⁻(NEt₄⁺)·(H₂O)** and 2.603(1) Å in **2′–O⁻(NMe₄⁺)**) suggest that all *N-tert*-butylcarbamoyl groups form an intramolecular NH · · · O(oxyanion) hydrogen bond. In the phenolate anions, no significant intermolecular interactions were observed, except for the short contact between the phenolate oxygen atom and the water oxygen in **1′–O⁻(NEt₄⁺)·(H₂O)**. Crystal structure of **1′OH** was also analyzed. However, it gives

Table 1 Selected short contacts, bond distance and torsion angles of **1–OH**, **2′–OH**, **1′–O⁻(NEt₄⁺)·H₂O** and **2′–O⁻(NMe₄⁺)**

	1–OH	**2′–OH**	**1′–O⁻(NEt₄⁺)·H₂O**	**2′–O⁻(NMe₄⁺)**	**1′–OH**
O11···O1	2.501(2)	2.461(4)	—	—	2.549(2)
(O11···O1* for **1′–OH**)	2.514(3)	2.471(4)	—	—	2.606(2)
					2.614(2)
O11···N2	—	2.673(4)	—	—	—
		2.654(4)			
O11···N1	—	—	2.690(4)	2.603(1)	2.598(2)
					2.652(2)
					2.661(2)
C11–O11	1.353(3)	1.341(4)	1.294(5)	1.307(2)	1.361(3)
	1.357(3)	1.352(4)			1.361(3)
					1.363(3)
C11–C12–C1–N1	−172.5(2)	−170.0(3)	14.9(6)	8.59(18)	2.1(3)
	169.2(2)	161.3(4)			−7.5(4)
					−11.9(4)
C11–C16–C2–N2	—	13.5(6)	—	—	—
		−7.2(6)			

less information about intramolecular hydrogen bond than **1–OH** because it forms an intermolecular OH···O=C hydrogen bond (Fig. 1e).

All structures showed small torsion angles (high coplanarity) between the aromatic and amide planes. The C11–O11 bond lengths in the phenolate anions were shorter than those in the corresponding phenols. This finding indicates that an increase in the double bond character of the phenolate anion occurred because of the delocalization of the negative charge on the anionic oxygen atom to the aromatic ring. These structural features are similar to the findings of our recent works.[12,13]

Solution structures

Intramolecular hydrogen-bond formation was confirmed by ¹H NMR measurement in acetonitrile-d_3 solution (5 mM, sufficiently dilute to neglect intermolecular interactions; experimental details are available in the supplementary information). The phenol and the phenolate anion with the *para-N-tert*-butyl carbamoyl group, **3–OH** and **3–O⁻(NEt₄⁺)**, were used as references without any intramolecular hydrogen bond. Chemical shifts of phenolic OH and amide NH protons are summarized in Table 2, and schematic drawings of the solution structures indicating the intramolecular hydrogen bonds are shown in Scheme 3. These chemical shifts are effective in determining the conformation of salicylamide derivatives. Hydrogen bonded phenolic OH signals in phenol and amide NH signals in phenolate anion were observed in an extremely low field (>11 ppm).[12,13] The phenolic OH signal of **1–OH** was observed at 13.18 ppm, indicating the formation of an intramolecular OH···O=C hydrogen bond. A similar hydrogen bond should be formed in **2–OH** although the OH signal of **2–OH** was not observed even at −30 °C, which is probably because of the proton exchange between the two *ortho*-substituents (Scheme 4). In the case of **2′–OH**, which is an analogous compound to **2–OH**, a broad singlet OH signal was observed in a very low field, 14.00 ppm. The amide NH signals of the phenolate anions, **1–O⁻(NEt₄⁺)**, **2–O⁻(NEt₄⁺)** and **3–O⁻(NEt₄⁺)**, were observed at 13.21, 11.92 and 5.74 ppm, respectively. The lower-field shifts of the NH signal strongly indicate the presence of the intramolecular NH···O(oxyanion) hydrogen bond. In acetonitrile solution, these phenols and phenolate anions favor a hydrogen-bonding mode similar to what is found in the crystal structures.

Contribution of hydrogen bonds to pK_a shift

The pK_a values in an aqueous micellar solution of **1′–OH**, **2′–OH**, **3′–OH** and **5′–OH**, which forms intramolecular OH···O=C and NH···O hydrogen bonds,[12] were determined by potentiometric titration to be 9.2, 7.5, 9.4 and 8.1, respectively, and are summarized in Fig. 2. In an aqueous micellar

Table 2 Chemical shifts of phenolic OH and amide NH protons, 5 mM in CD₃CN

	OH	NH	
	δ/ppm (**OH**)	δ/ppm (**OH**)	δ/ppm (**O⁻(NEt₄⁺)**)
1–	13.18	6.80	13.21
2–	Not observed[a]	7.81	11.92
3–	5.75	6.41	5.74

[a] Even at −30 °C.
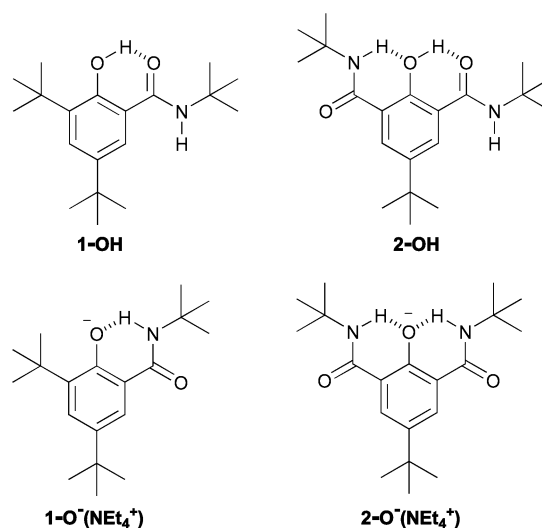
Scheme 3 Solution structures of **1–OH**, **2–OH**, anion of **1–O⁻(NEt₄⁺)** and anion of **2–O⁻(NEt₄⁺)**.
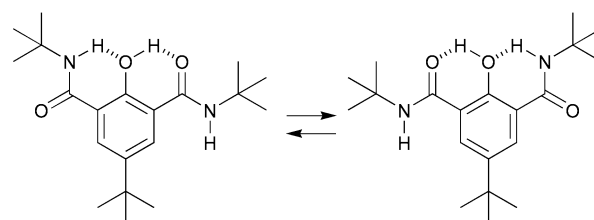
Scheme 4 Proton exchange on **2–OH** in solution.

solution consisting of two heterogeneous layers, hydrophobic and hydrophilic, the phenols are buried in the hydrophobic layer, where the intramolecular hydrogen bonds discussed above are supported. Under these conditions, pK_a values are verified as accurate in hydrophobic environments like the inside of a protein (not in a mixture of aqueous and organic media) because of
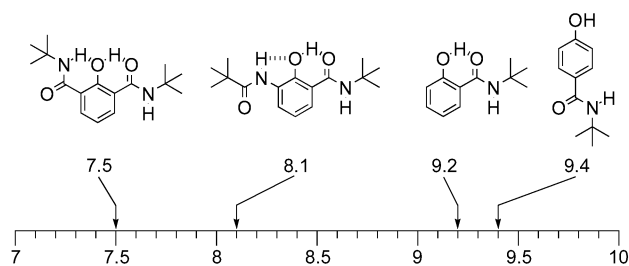
Fig. 2 Summary of pK_a values.

rapid proton transfer between two layers.[14,15] The OH···O=C and NH···O hydrogen bonds in the model compounds are regarded as simulating the OH···N and OH(water)···O hydrogen bonds in PSII (Scheme 1), respectively. It has been reported that salicylamide derivatives show a low pK_a value due to the NH···O(oxyanion) hydrogen bond in both aqueous and dimethylacetamide solutions,[16] where the intramolecular OH···O=C hydrogen bond is not supported and the existence of NH···O–hydrogen bonded conformer has been proposed as a result of intermolecular hydrogen bonding with solvent molecules (similar conformation to the crystal structure of **1'–OH** (Fig. 1e). On the other hand, in an aqueous micellar solution **1'–OH** showed a negligible pK_a shift from that of **3'–OH**, which has similar electronic effects of the *N*-*tert*-butylcarbamoyl group to **1'–OH**. In an aqueous micellar solution, NH···O–hydrogen bonded conformer does not exist because the intramolecular OH···O=C hydrogen bond is supported under these conditions. These results indicate that lowering the pK_a value of salicylamide derivatives is due to not the formation of NH···O(oxyanion) hydrogen bond in the phenolate anion but the formation of NH···O hydrogen bond from pre-locating NH to the phenolic hydroxyl group in the deprotonation process. The OH···O=C hydrogen bond in **1'–OH** does not raise the pK_a value, in contrast to a process proposed for the OH···O(carboxylate) hydrogen bond in salicylate mono-anions.[17] This is probably due to the difference of hydrogen-accepting abilities between carbonyl and carboxylate groups. The energy barrier of a local proton transfer between phenolic and carbonyl oxygen atoms should be low, as observed in the two-centered short hydrogen bonds.[18] The phenols, **2'–OH** and **5'–OH**, which form the NH···O hydrogen bond adding to the OH···O=C hydrogen bond, showed lower pK_a values. These pK_a shifts also indicate the contribution of the pre-locating NH, and similar shifts were found in our previous results on phenols,[14] thiophenols[19] and benzoic acids.[15] Lowering pK_a values by pre-locating hydrogen-bonding donor is important in terms of the shift of the acid–base equilibrium between the tyrosine and histidine residues to a more polarized state. In PSII, the hydrogen bonded water presumably plays an important role not only in the reduction of the tyrosyl radical as a hydrogen source,[20] but also in lowering the pK_a value.

Contribution of hydrogen bonding to the shift of oxidation potential

The oxidation potential of phenols **1–OH** to **5–OH** and phenolate anions **1–O⁻(NEt₄⁺)** to **5–O⁻(NEt₄⁺)** were measured in acetonitrile. In all of the phenols and phenolate anions, including related compounds,[21,22] two substituents with a similar bulkiness were introduced to the *ortho*-positions because the bulkiness at these positions has been reported to affect the redox potentials of the phenolate anion.[22] Hammett constants, σ^+, for CONH-*t*-Bu and NHCO-*t*-Bu have not been reported, thus alternative values for COOEt and NHCOMe were used, respectively.[23] The electronic effect of an *ortho*-substituent is related to that of a *para*-substituent in (4).[24]

$$\sigma_o^+ = 0.66\,\sigma_p^+ \tag{4}$$

Table 3 Oxidation potentials of phenol and phenolate anion derivatives and sum of Hammett constants

	E_{pa}/V (**OH**)	E_{pa}/V (**O⁻(NEt₄⁺)**)	$\Sigma\sigma^+$
1–	1.45	0.24	−0.11
2–	1.53	0.58	0.37
3–	1.61	0.04	0.14
4–	1.25	−0.05	−0.83
5–	1.57	0.31[a]	0.34
2,4,6-(t-Bu)$_3$C$_6$H$_2$–	1.50[b]	−0.23[b]	−0.60
2,6-(t-Bu)$_2$C$_6$H$_2$–	1.54	−0.19[c,d]	−0.34
2,6-(t-Bu)$_2$-4-MeC$_6$H$_2$–	1.44[b]	−0.35[b]	−0.65
2,6-(t-Bu)$_2$-4-MeOC$_6$H$_2$–	1.16[b]	−0.40[b]	−1.12
4-Br-2,6-(t-Bu)$_2$C$_6$H$_2$–	1.49	−0.03[c]	−0.19

[a] Ref. 12. [b] Ref. 21. [c] Ref. 22 (tetramethylammonium salt). [d] Oxidation potential is slightly more positive (*ca.* +0.05 V) than this value because the value is given as a redox potential.
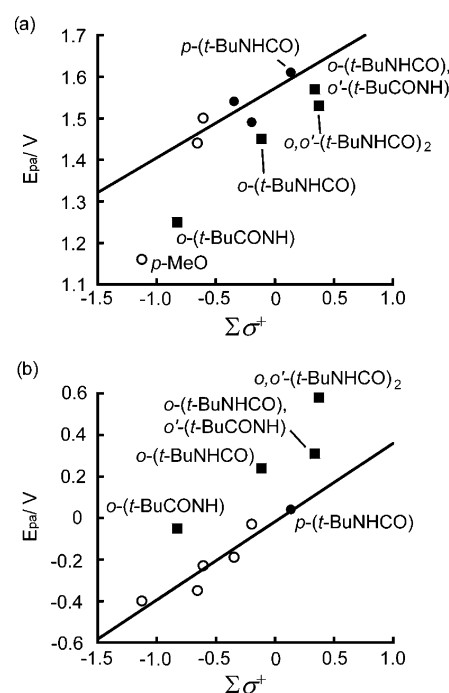

Fig. 3 Correlation of oxidation potential with sum of Hammett constants, (a) phenols and (b) phenolate anions. Solid circles and squares are our results, including ref. 12, and open circles are from ref. 21 and ref. 22. Squares are plots for hydrogen bonded compounds and circles are the other. All the phenols and phenolate anions have *tert*-butyl groups at the *ortho*- and *para*-positions if not specified in the plots.

The oxidation potentials and the sum of the electronic effects of the substituents, $\Sigma\sigma^+$, are summarized in Table 3. The plot of the oxidation potentials of the phenol against $\Sigma\sigma^+$ is shown in Fig. 3a. Non-hydrogen bonded phenols, with the exception of 2,6-di-*tert*-butyl-4-methoxyphenol, show good linearity. The deviation of the oxidation potential of 2,6-di-*tert*-butyl-4-methoxyphenol is attributed to the stabilization of the corresponding radical with the favorable resonance structure by the 4-methoxy group.[25] The overall trend (with one minor exception) is that the hydrogen bonded phenols show a relatively negative oxidation potential compared with the non-hydrogen bonded ones. The formation of an intramolecular OH···O=C hydrogen bond in **4–OH** was indicated by the crystal structure of the **4–OH** analogue, bis-(3,5-di-*tert*-butyl-2-phenol)-oxamide (Scheme 5).[26] In the case of **2–OH** and **5–OH**, the formation of another intramolecular hydrogen bond, NH···O(phenol), was suggested by the crystal structures. However, an additional shift of the oxidation potential caused by the NH···O(phenol) hydrogen bond was not observed. This type of hydrogen bond, where phenolic oxygen acts as a hydrogen bond acceptor, has
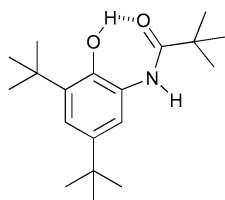
Scheme 5 Predominant solution structure of **4–OH**.

been reported to contribute to the high antioxidant activity of phenol by lowering the bond dissociation enthalpy of the O–H bond.[27,28] The inconsistency is probably due to the fact that electrochemical oxidation in this study did not include the O–H bond dissociation. The contribution of the intramolecular OH $\cdots$ O=C hydrogen bond to the oxidation potential of phenol is similar to the reported results that the OH $\cdots$ N(amine) hydrogen bond, where the phenolic hydroxyl group acts as a hydrogen-bonding donor, negatively shifts the redox potential of the phenol (*ca.* 0.7–1.1 V).[9–11,29] However, the effect is relatively small and vague because the basicity of carbonyl oxygen is lower than that of amino nitrogen in the other studies.

A similar plot for phenolate anions is shown in Fig. 3b. Non-hydrogen bonded phenolate anions show a good linearity in the correlation as reported previously.[22] On the other hand, all of the hydrogen bonded phenolate anions show more positive oxidation potentials than expected from the sum of electronic effects. The results indicate that the intramolecular NH $\cdots$ O(oxyanion) hydrogen bonds positively shift the oxidation potential of the phenolate anion. A positive shift caused by the double NH $\cdots$ O(oxyanion) hydrogen bond in **2–O$^-$ (NEt$_4^+$)** and **5–O$^-$ (NEt$_4^+$)** is comparable to that caused by a single hydrogen bond in **1–O$^-$ (NEt$_4^+$)** and **4–O$^-$ (NEt$_4^+$)**.

### Protection by NH $\cdots$ O(oxyanion) hydrogen bond from oxidation by dioxygen

The shift in oxidation potential of the phenolate anion caused by the presence of NH $\cdots$ O(oxyanion) hydrogen bonds may be of biological importance in another aspect. In nature, there are phenolate anions, such as phenolic chromophores in photoactive yellow protein (PYP)[30] and green fluorescent protein (GFP)[31] that are rarely oxidized. If these phenolate anions have typical oxidation potentials for phenolate anions, they should be easily oxidized by dioxygen. It is possible that they are protected from oxidation by hydrogen bonds to the phenolate anions proposed in proteins. From this viewpoint, the oxidation of phenolate anions by dioxygen was examined using **1–O$^-$ (NEt$_4^+$)**, **2–O$^-$ (NEt$_4^+$)** and **3–O$^-$ (NEt$_4^+$)**. Introduction of quantified excess dioxygen into the acetonitrile solution containing **1–O$^-$ (NEt$_4^+$)** and **3–O$^-$ (NEt$_4^+$)** resulted in a decrease in the absorption band at 350 and 332 nm, respectively, which indicates oxidation of the phenolate anions (Fig. 4).[32,33] In a dioxygen atmosphere, **3–O$^-$ (NEt$_4^+$)** was almost completely oxidized after 2 d. However, only *ca.* 10% of **1–O$^-$ (NEt$_4^+$)** was oxidized under the same conditions. In the case of **2–O$^-$ (NEt$_4^+$)**, the absorption spectrum did not show a meaningful change for at least 2 d (Fig. 5 shows the UV-vis spectrum of **2–O$^-$ (NEt$_4^+$)**). The positive oxidation potential shift caused by the NH $\cdots$ O(oxyanion) hydrogen bonds results in an increased stability of the phenolate anions against oxidation by dioxygen. The hydrogen bonds to phenolate anion in PYP, GFP and other proteins also prevent the oxidation of the phenolate anions by dioxygen.

Conclusions

The intramolecular OH $\cdots$ O=C, NH $\cdots$ O(phenol), and NH $\cdots$ O(oxyanion) hydrogen bonds in phenols and phenolate anions were established through crystallographic analyses and ^{1}H NMR spectroscopic results. In phenol, the intramolecular NH $\cdots$ O(phenol) hydrogen bond from pre-located NH lowers
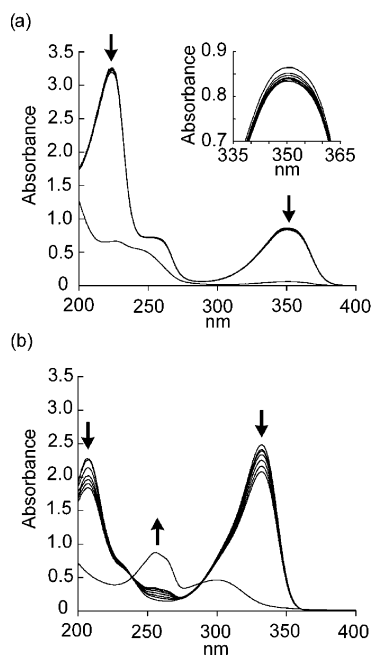

Fig. 4 UV-vis spectral changes in the reaction of (a) **1–O$^-$ (NEt$_4^+$)** and (b) **3–O$^-$ (NEt$_4^+$)** with dioxygen in acetonitrile at 298 K (60 min interval spectra, after 7 weeks for **1–O$^-$ (NEt$_4^+$)** and 1 week for **3–O$^-$ (NEt$_4^+$)**).
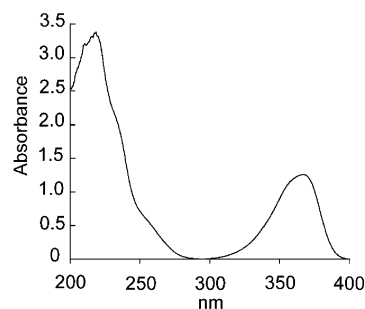
Fig. 5 UV-vis spectrum of **2–O$^-$ (NEt$_4^+$)** in acetonitrile at 298 K.

the pK_a value of the phenolic OH group. The intramolecular OH $\cdots$ O=C hydrogen bond negatively shifts the oxidation potential of the phenol. In contrast, another NH $\cdots$ O(phenol) hydrogen bond in **2–OH** and **5–OH** shows a negligible additional shift of the oxidation potential. The intramolecular NH $\cdots$ O(oxyanion) hydrogen bonds positively shift the oxidation potential of the phenolate anion.

Based on these results, the role of hydrogen bonds in PSII can be considered. The hydrogen bond between the tyrosine and histidine residues finely adjusts the oxidation potential of the tyrosine to an adequate value for electron transfer (Fig. 6). It also decreases the energy barrier of a local proton transfer between the tyrosine and histidine residues. The hydrogen bond between the tyrosine residue and water lowers the pK_a of the phenolic OH group. Lowering the pK_a value is important in terms of shifting the acid–base equilibrium between the tyrosine and histidine residues to a more polarized state, resulting in an increased
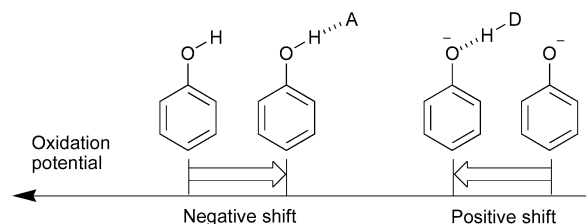
Fig. 6 Schematic diagram of shift of oxidation potentials by hydrogen bonds (OH $\cdots$ A and DH $\cdots$ O(oxyanion)). A and DH represent a hydrogen-bond acceptor and donor, respectively.

anionic character of the tyrosine. In PSII, the hydrogen bonded water is important not only in the reduction of the tyrosyl radical as a hydrogen source but also in terms of lowering the pK_a of the tyrosine.

The hydrogen bond to a phenolate anion greatly shifts the oxidation potential of the phenolate anion. Based on this finding, the reaction rate of oxidation by dioxygen is remarkably reduced. These results indicate that the phenolate anions in PYP, GFP and other proteins (tyrosinate anions certainly exist in various proteins even if they have been seldom noted) are probably protected from oxidation by the presence of hydrogen bonds formed to the phenolate anion.

Experimental

pH titration

The pH of 10 mM solution of each phenol was determined using a Metrohm 716 DMS titrino combined with a Metrohm 728 stirrer and a saturated calomel LL micro pH glass electrode. The saturated calomel micro glass electrode was calibrated with the 0.05 M KHC$_6$H$_4$(COO)$_2$ buffer (pH = 4.01) and the 0.025 M KH$_2$PO$_4$–Na$_2$HPO$_4$ buffer (pH = 6.86) at 30 °C. The sample was dissolved in a small amount of THF and to the solution was added Triton X-100. After removal of THF under reduced pressure, the obtained residue was diluted with degassed water to give a micellar solution. The final concentration is 10% Triton X-100 aqueous solution containing 10 mM of the sample. The solution was titrated with 0.1 M NaOH aq. at 30 °C. The pK_a value was estimated by the following equation: pK_a = pH − log[Na$^+$] + log{[phenol]$_0$ − [Na$^+$]}.

Oxidation by dioxygen

To dioxygen-purged UV cell (volume, 6 mL; light path length, 10 mm) was added 2 mL of acetonitrile solution containing 0.1 mM of the samples. After shaking for 30 seconds, the cell was stored at 25 °C. UV-vis spectral change was monitored using a SHIMADZU UV-3100PC spectrophotometer.

X-Ray structure determination

Each single crystal of **1′–OH**, **1′–O⁻(NEt₄⁺)** and **2′–OH** was sealed in a glass capillary and **1–OH** and **2′–O⁻(NMe₄⁺)** were mounted in a loop with Nujol. The X-ray data of **1′–OH**, **1′–O⁻(NEt₄⁺)** and **2′–OH** were collected at 298 K on a Rigaku AFC7R diffractometer and those of **1–OH** and **2′–O⁻(NMe₄⁺)** were collected at 200 K on a Rigaku Raxis-RAPID Imaging Plate diffractometer with graphite monochromated Mo Kα (λ = 0.71069 Å). The structure was solved by the direct method (SIR92[34] for **1–OH**, **1′–OH** and **2′–O⁻(NMe₄⁺)** and MULTAN88[35] for **1′–O⁻(NEt₄⁺)** and SHELXS-97[36] for **2′–OH**) and expanded using Fourier techniques using teXsan crystallographic software[37] and SHELXL-97.[38] Non-hydrogen atoms were refined anisotropically. The hydrogen atoms were placed at calculated positions.

Crystal data for 1–OH‡. C$_{19}$H$_{31}$NO$_2$, M = 305.45, triclinic, space group $P\bar{1}$, a = 10.6747(6), b = 12.0073(3), c = 15.3190(11) Å, α = 101.634(3)°, β = 99.209(4)°, γ = 90.717(4)°, V = 1896.34(18) Å^3, Z = 4, μ(Mo–Kα) = 0.068 mm^{-1}, 8344 reflections measured, 4113 unique (R_{int} = 0.064), R_1 = 0.078, wR_2 = 0.248 (all data). CCDC reference number 259697.

Crystal data for 2′–OH‡. C$_{16}$H$_{24}$N$_2$O$_3$, M = 292.37, triclinic, space group $P\bar{1}$, a = 12.233(4), b = 13.207(4), c = 11.841(4) Å, α = 105.46(2)°, β = 109.07(3)°, γ = 90.81(3)°, V = 1732.0(10) Å^3, Z = 4, μ(Mo–Kα) = 0.078 mm^{-1}, 5813 reflections measured,

5561 unique (R_{int} = 0.063), R_1 = 0.061, wR_2 = 0.227 (all data). CCDC reference number 259700.

Crystal data for 1′–O⁻(NEt₄⁺)·H₂O‡. C$_{19}$H$_{34}$N$_2$O$_2$·H$_2$O, M = 340.50, triclinic, space group $P\bar{1}$, a = 10.0678(16), b = 12.211(3), c = 9.0829(12) Å, α = 97.147(15)°, β = 92.285(15)°, γ = 109.753(14)°, V = 1038.8(3) Å^3, Z = 2, μ(Mo–Kα) = 0.073 mm^{-1}, 5729 reflections measured, 4752 unique (R_{int} = 0.035), R_1 = 0.069, wR_2 = 0.277 (all data). CCDC reference number 259699.

Crystal data for 2′–O⁻(NMe₄⁺)‡. C$_{20}$H$_{35}$N$_3$O$_3$, M = 365.51, orthorhombic, space group $Cmc2_1$, a = 13.2912(6), b = 13.0775(5), c = 12.1094(5) Å, V = 2104.80(15) Å^3, Z = 4, μ(Mo–Kα) = 0.078 mm^{-1}, 2451 reflections measured, 2171 unique (R_{int} = 0.036), R_1 = 0.039, wR_2 = 0.093 (all data). CCDC reference number 259701.

Crystal data for 1′–OH‡. C$_{11}$H$_{15}$NO$_2$, M = 193.24, monoclinic, space group $P2_1$/c, a = 14.266(6), b = 12.599(4), c = 19.587(4) Å, β = 100.86(2)°, V = 3457.3(18) Å^3, Z = 12, μ(Mo–Kα) = 0.077 mm^{-1}, 7518 reflections measured, 7197 unique (R_{int} = 0.055), R_1 = 0.048, wR_2 = 0.159 (all data). CCDC reference number 259698.

Acknowledgements

References

1 R. P. Pesavento and W. A. Van Der Donk, *Adv. Protein Chem.*, 2001, **58**, 317–385.
2 J. Stubbe and W. A. van der Donk, *Chem. Rev.*, 1998, **98**, 705–762.
3 K. K. Andersson, P. P. Schmidt, B. Katterle, K. R. Strand, A. E. Palmer, S.-K. Lee, E. I. Solomon, A. Graeslund and A.-L. Barra, *JBIC, J. Biol. Inorg. Chem.*, 2003, **8**, 235–247.
4 P. Dorlet, S. A. Seibold, G. T. Babcock, G. J. Gerfen, W. L. Smith, A.-L. Tsai and S. Un, *Biochemistry*, 2002, **41**, 6107–6114.
5 A. Ivancich, G. Mazza and A. Desbois, *Biochemistry*, 2001, **40**, 6860–6866.
6 P. J. van Dam, J.-P. Willems, P. P. Schmidt, S. Pötsch, A.-L. Barra, W. R. Hagen, B. M. Hoffman, K. K. Andersson and A. Gräslund, *J. Am. Chem. Soc.*, 1998, **120**, 5080–5085.
7 S. Un, M. Atta, M. Fontecave and A. W. Rutherford, *J. Am. Chem. Soc.*, 1995, **117**, 10713–10719.
8 L. Sun, M. Burkitt, M. Tamm, M. K. Raymond, M. Abrahamsson, D. LeGourriérec, Y. Frapart, A. Magnuson, P. H. Kenez, P. Brandt, A. Tran, L. Hammarström, S. Styring and B. Åkermark, *J. Am. Chem. Soc.*, 1999, **121**, 6834–6842.
9 T. Maki, Y. Araki, Y. Ishida, O. Onomura and Y. Matsumura, *J. Am. Chem. Soc.*, 2001, **123**, 3371–3372.
10 F. Thomas, O. Jarjayes, C. Duboc, C. Philouze, E. Saint-Aman and J.-L. Pierre, *Dalton Trans.*, 2004, 2662–2669.
11 I. J. Rhile and J. M. Mayer, *J. Am. Chem. Soc.*, 2004, **126**, 12718–12719.
12 D. Kanamori, T. Okamura, H. Yamamoto and N. Ueyama, *Angew. Chem., Int. Ed.*, 2005, **44**, 969–972.
13 D. Kanamori, T. Okamura, H. Yamamoto, S. Shimizu, Y. Tsujimoto and N. Ueyama, *Bull. Chem. Soc. Jpn.*, 2004, **77**, 2057–2064.
14 D. Kanamori, Y. Yamada, A. Onoda, T. Okamura, S. Adachi, H. Yamamoto and N. Ueyama, *Inorg. Chim. Acta*, 2005, **358**, 85–92.
15 A. Onoda, Y. Yamada, J. Takeda, Y. Nakayama, T. Okamura, M. Doi, H. Yamamoto and N. Ueyama, *Bull. Chem. Soc. Jpn.*, 2004, **77**, 321–329.
16 W. L. Mock and D. C. Y. Chua, *J. Chem. Soc., Perkin Trans. 2*, 1995, 2069–2074.
17 W. L. Mock and L. A. Morsch, *Tetrahedron*, 2001, **57**, 2957–2964.
18 J. Chen, M. A. McAllister, J. K. Lee and K. N. Houk, *J. Org. Chem.*, 1998, **63**, 4611–4619.
19 N. Ueyama, M. Inohara, A. Onoda, T. Ueno, T. Okamura and A. Nakamura, *Inorg. Chem.*, 1999, **38**, 4028–4031.
20 C. Tommos and G. T. Babcock, *Biochim. Biophys. Acta*, 2000, **1458**, 199–219.

‡ CCDC reference numbers 259697–259701. See http://www.rsc.org/suppdata/ob/b4/b419361j/ for crystallographic data in .cif format.

21 L. L. Williams and R. D. Webster, *J. Am. Chem. Soc.*, 2004, **126**, 12441–12450.

22 P. Hapiot, J. Pinson and N. Yousfi, *New J. Chem.*, 1992, **16**, 877–881.

23 C. Hansch, A. Leo and R. W. Taft, *Chem. Rev.*, 1991, **91**, 165–195.

24 M. Jonsson, J. Lind, T. E. Eriksen and G. Merényi, *J. Chem. Soc., Perkin Trans. 2*, 1993, 1567–1568.

25 F. G. Bordwell, X.-M. Zhang, A. V. Satish and J. P. Cheng, *J. Am. Chem. Soc.*, 1994, **116**, 6605–6610.

26 V. M. Jímenez-Pérez, C. Camacho-Camacho, M. Güizado-Rodríguez, H. Nöth and R. Contreras, *J. Organomet. Chem.*, 2000, **614–615**, 283–293.

27 R. Amorati, M. Lucarini, V. Mugnaini and G. F. Pedulli, *J. Org. Chem.*, 2003, **68**, 5198–5204.

28 M. Lucarini, G. F. Pedulli and M. Guerra, *Chem. Eur. J.*, 2004, **10**, 933–939.

29 L. Benisvy, A. J. Blake, D. Collison, E. S. Davies, C. D. Garner, E. J. L. McInnes, J. McMaster, G. Whittaker and C. Wilson, *Dalton Trans.*, 2003, 1975–1985.

30 M. Baca, G. E. O. Borgstahl, M. Boissinot, P. M. Burke, D. R. Williams, K. A. Slater and E. D. Getzoff, *Biochemistry*, 1994, **33**, 14369–14377.

31 M. Ormö, B. Cubitt, K. Kallio, L. A. Gross, R. Y. Tsien and S. J. Remington, *Science*, 1996, **273**, 1392–1395.

32 I. Nakanishi, K. Miyazaki, T. Shimada, Y. Iizuka, K. Inami, M. Mochizuki, S. Urano, H. Okuda, T. Ozawa, S. Fukuzumi, N. Ikota and K. Fukuhara, *Org. Biomol. Chem.*, 2003, **1**, 4085–4088.

33 I. Nakanishi, K. Fukuhara, K. Ohkubo, T. Shimada, H. Kansui, M. Kurihara, S. Urano, S. Fukuzumi and N. Miyata, *Chem. Lett.*, 2001, 1152–1153.

34 A. Altomare, M. C. Burla, M. Camalli, M. Cascarano, C. Giacovazzo, A. Guagliardi and G. Polidori, *J. Appl. Crystallogr.*, 1994, **27**, 435.

35 T. Debaerdemaeker, G. Germain, P. Main, L. S. Refaat, C. Tate and M. M. Woolfson, *MULTAN88: Computer programs for the automatic solution of crystal structures from X-ray diffraction data*, University of York, UK, 1988.

36 G. M. Sheldrick, *SHELXS-97, Program for solution of crystal structures*, University of Göttingen, Germany, 1997.

37 *teXsan: Crystal Structure Analysis Package*, Molecular Structure Corporation, 1985 and 1992.

38 G. M. Sheldrick, *SHELXL-97, Program for refinement of crystal structures*, University of Göttingen, Germany, 1997.